Influence of microstructure and applied current on the electrical conductivity of $SmBaCo_2O_{5+d}$ cathode in solid oxide fuel cell

Kyeong Eun Song [a], Jae Woong Lee [a], Yu Ri Lim [a], Seung Wook Baek [b], Tae Ho Shin [c], Shin Ku Lee [d], Harald Schlegl [e], Jung Hyun Kim [a,*]

[a] Department of Advanced Materials Science and Engineering, Hanbat National University, 125, Dongseo-Daero, Yuseong-Gu, Daejeon, 34158, Republic of Korea

[b] Interdisciplinary Materials Measurement Institute, Korea Research Institute of Standards and Science (KRISS), 267, Gajeong-Ro, Yuseong-Gu, Daejeon, 34113, Republic of Korea

[c] Korea Institute of Ceramic Engineering and Technology, Energy and Environmental Division, 101, Soho-Ro, Jinju-Si, Gyeongsangnam-Do, 52851, Republic of Korea

[d] HnPower, Inc. Factory: 129, Techno 2-Ro, Yuseong-Gu, Daejeon, Republic of Korea, HQ/R&D Center: N9-4160 KAIST, 291, Daehak-Ro, Yuseong-Gu, Daejeon, Republic of Korea

[e] Chemistry Department, Lancaster University, Bailrigg, Lancaster LA1 4YB, United Kingdom

Corresponding author:*

Jung Hyun Kim: jhkim2011@hanbat.ac.kr, jhkim1870@gmail.com,

Tel: +82-42-821-1239, Fax: +82-42-821-1592,

Department of Advanced Materials Science and Engineering, Hanbat National University, 125,

Dongseo-Daero, Yuseong-Gu, Daejeon, 34158, Republic of Korea

Abstract

In this study, the electrical conductivity of $SmBaCo_2O_{5+d}$ (SBCO) is measured and analyzed with respect to the microstructure of the analyzed samples. The microstructure is influenced by the sintering temperature and by the precise composition of the composite cathode. Difference in the electrical conductivity at different applied current is investigated. The value of the electrical conductivity of SBCO sintered at 1150 ºC was about 1024 S/cm at 600 ºC, which was the highest compared to other samples sintered at lower temperatures. The electrical conductivities of porous microstructural SBCO sintered at 1150 ºC with an addition of 10 wt% carbon black and of a composite cathode comprised of SBCO and $Ce_{0.9}Gd_{0.1}O_2$ (CGO91) at a ratio of 1.9:0.1 were 256 and 525 S/cm at 600 ºC. The electrical conductivities of SBCO samples increase when relatively low currents are applied. This trend can be observed at all pure SBCO and samples mixed with carbon black. However, these properties are not found in composite cathodes comprised of SBCO and CGO91.

Keywords: Intermediate Temperature-operating Solid Oxide Fuel Cell (IT-SOFC), Cathode, Electrical Conductivity, Layered Perovskite, Microstructure.

Introduction

Solid Oxide Fuel Cells (SOFCs) are energy devices that generate electrical energy directly from the chemical energy of oxygen and fuel gases like hydrogen, methane or the reformates of higher hydrocarbons. SOFCs have the advantages of high efficiency, low carbon emissions and fuel flexibility due to their high operating temperature (500 ~ 1000 ^{o}C) and materials used [1-7]. The single cell in SOFCs consists of cathode, electrolyte and anode. Especially, the cathode is often the part that determines the performance of SOFCs, because typically around 50% of the total polarization resistance stems from the cathode [8-11]. To summarize the electrochemical properties of cathode materials, the oxygen reduction reaction (ORR) affects the cathode performance at the surface. The better the electron and ionic conductivity, the better the reduction reaction of oxygen molecules. On the other hand, the low electrical conductivity of the cathode reduces the efficiency of the electrochemical reaction [12, 13].

When the ionic conductivity is extremely low in cathode materials, the availability of ions generated through the ORR reaction is limited to the interface between the electrolyte and the cathode because of a lack of ion mobility, which leads to a decrease in efficiency and performance as the reaction active sites become insufficient. In addition to conductivity-dependent properties, SOFCs show differences in electrochemical properties depending on the lattice structure of cathodes [14-16]. For example, perovskite oxide materials showing the complex perovskite structure can display a wide variation of physical and chemical characteristics depending on the degree of atomic substitution of each lattice site. By optimization of these characteristics, it is possible to improve not only physical properties but also electrochemical properties [17].

However, when various materials are substituted, dislocations according to the coulomb potential and elastic potential act on the cathode lattice due to disorder, preventing oxygen ion

movement [18]. To solve these problems, many researchers have focused on the development of layered perovskites having a chemical composition of $AA^{/}B_2O_{5+d}$ (A: lanthanide Ln, $A^{/}$: Ba or Sr, B: Co) as cathode materials for SOFCs [20-27]. In layered perovskite, specific crystallographic characteristics have been reported in the case of Ba substituted for the A-site. For example, when Ba is substituted into the $A^{/}$-site, a crystal structure is formed according to the staking $[CoO_2]$-[BaO]-$[CoO_2]$-$[LnO_6]$ layers [19]. Especially in layered perovskites, this material has excellent oxygen mobility and surface kinetics due to many vacancies in the lattice structure, because of oxygen atoms are removed partially or completely in the [Ln-O_6] layer [17]. Table 1 summarizes the characteristics of the $LnBaCo_2O_{5+d}$ composition of layered perovskite cathode materials. Many research groups reported that the cathode of SOFCs show excellent electrochemical properties whenever the cathode material displays high electrical conductivity [20-27].

Chemical compositions	Properties	Refer.
$GdBaCo_2O_{5+d}$	▪ Electrical conductivity 655 and 163 S/cm at 100 and 900 ºC	[20]
$PrBaCo_2O_{5+d}$	▪ Electrical conductivity 1323 and 310 S/cm at 100 and 900 ºC ▪ Area Specific Resistance (ASR) 0.233 Ωcm^2 at 700 °C	[21]
$SmBaCo_2O_{5+d}$	▪ Electrical conductivity 570 and 170 S/cm at 250 and 900 ºC ▪ Area Specific Resistance (ASR) 0.131 Ωcm^2 at 700 ºC	[21, 22]
$LaBa_{0.5}Sr_{0.5}Co_{1.5}Fe_{0.5}O_{5+d}$	▪ Electrical conductivity 1400 S/cm at 400 ºC	[23]
$PrBaCuCoO_{5+d}$	▪ ASR values	[24]

	0.047 Ωcm^2 at 700 °C	
$NdBa_{0.5}Sr_{0.5}CoO_{5+d}$	▪ Electrical conductivity 51.92 S/cm at 545 °C	[25]
$SmBa_{0.8}Ca_{0.2}Co_2O_{5+d}$	▪ Electrical conductivity 329.7 S/cm at 700 ºC ▪ Area Specific Resistance (ASR) 0.26 Ωcm^2 at 700°C	[26]
$Sm_{0.2}Nd_{0.8}Ba_{0.5}Sr_{0.5}Co_2O_{5+d}$	▪ Electrical conductivity 1280 and 280 S/cm at 50 °C and 900 °C ▪ Area Specific Resistance (ASR) 0.244 and 0.044 Ωcm^2 at 600 and 700 °C	[27]

Table 1. Layered barium cobaltate perovskites with different lanthanide substitution at the A-site and their electrochemical benefits in literature

The electrical conductivities displayed in Table 1 have been generally measured through experimental conditions using dense sample. However, in actual cathodes of SOFCs, half-cell and single cell experiments are performed using porous samples to ensure smooth gas diffusion and a well developed triple phase boundary (TPB) [28, 29]. In other words, the values and behaviors of electrical conductivity have been known to be inherent properties and were measured in samples with a dense microstructure. However, all electrochemical properties such as area specific resistance (ASR) and power density are observed in samples having porous microstructures [29, 30]. Therefore, for proper comparison and evaluation of overall conductivity, the porosity and pore microstructure of a perovskite sample used as the SOFCs cathode has to be taken into consideration as well as its chemical composition. Two samples with exactly identical chemical composition might still display values for conductivity differing by several orders of magnitude if porosity and microstructure are different. Based on

these research objectives, our research group investigated the electrical conductivity properties of $SmBaCo_2O_{5+d}$ (SBCO) layered perovskites as a function of microstructural changes.

In this study, the electrical conductivity characteristics of SBCO with changes in microstructure after using various sintering temperatures, addition of carbon black and $Ce_{0.9}Gd_{0.1}O_{2-d}$ (CGO91) were analyzed. In addition, the current-voltage-power (I-V-P) curve is a method to measure the electrochemical properties of the SOFCs as a function of current density in the various ranges. Electrical conductivity is affected by different applied current density values, but generally published research papers report the electrical conductivity values and characteristics at only one specific applied current [17, 22, 31]. Taking into consideration the influence of both microstructure of the cathode and the current density at the cathode, the characteristics of the electrical conductivity of SBCO providing different preparation conditions leading to different sample microstructure and different applied current were simultaneously investigated in this study.

2. Experimental

2.1. Sample preparation and synthesis

Samarium Oxide (Sm_2O_3, 99.9%, Alfa Aesar), Barium Carbonate ($BaCO_3$, 99.8%, Alfa Aesar) and Cobalt Oxide (Co_3O_4, 99.7%, Alfa Aesar) powder were used for the synthesis of $SmBaCo_2O_{5+d}$ (SBCO) layered perovskite oxide system by solid state reaction (SSR). Each powder was accurately weighed according to its chemical composition, and mixed using an agate mortar with a pestle and ethanol. The powder mixtures were placed in an oven and maintained at 78 °C for 12 hours to evaporate the ethanol. Mixtures were calcined for 6 hours at 1000 °C with ramping rate of 5^oC/min as a first calcination step. After that, materials were

crushed, then, a secondary calcination step was carried out for 8 hours in an electric furnace at 1100 °C with ramping rate of 5 ºC/min in air atmosphere [17].

X-ray diffraction (XRD) patterns of the synthesized SBCO powder were obtained on a Model D/Max 2500, Rigaku (45Kv, 200mA, Cu kα radiation).

2.2 Electrical conductivity analysis

2.2.1 $SmBaCo_2O_{5+d}$ (SBCO) specimens for electrical conductivity

$SmBaCo_2O_{5+d}$ (SBCO) pellets for the measurement of electrical conductivity were prepared by pressing 2 x 10^3 kg/m^2 of rectangular-shaped bars (25 mm x 6 mm x 4 mm).

Then, pellets were sintered at 1000 °C, 1050 °C, 1100 °C or 1150 °C for 3 hours.

The sintering temperatures and abbreviations of the different SBCO samples for use as cathode materials are summarized in Table 2.

Sintering Temperature (ºC)	Abbreviation
1000	SBCO_1000
1050	SBCO_1050
1100	SBCO_1100
1150	SBCO_1150

Table 2. Abbreviations of SBCO samples sintered at the various temperatures

2.2.2 $SmBaCo_2O_{5+d}$ (SBCO) with 10wt% Carbon black specimens for electrical conductivity

To research electrical conductivity of samples with an advanced porous microstructure, 10 wt% carbon black was mixed with SBCO_1150 powder (showing the highest electrical conductivity of the samples fabricated at various sintering temperatures) and with SBCO_1000 powder (showing the lowest electrical conductivity of the samples fabricated at various sintering temperatures) powder. Carbon black was selected as a representative pore former because it can form small, uniform, and spherical pores [32, 33]. Rectangular bars with the dimensions 25 mm x 6 mm x 4 mm were prepared by pressing SBCO10C_1150 and SBCO10C_1000 mixtures with a pressure of 2 x 10^3 kg/m^2 and sintering them at 1150 ºC and 1000 ºC. However, the composite cathode heat-treated at 1000 ºC was not completely sintered and showed insufficient mechanical stability for conductivity tests, instead a sample bar sintered at 1050 ºC, SBCO10C_1050 was prepared and used for the testing procedure.

The sintering temperatures and abbreviations in SBCO with additional 10 wt% carbon black of cathode materials are summarized in Table 3.

Sintering temperature (ºC)	Abbreviation
1050	SBCO10C_1050
1150	SBCO10C_1150

Table 3. Abbreviations of SBCO samples sintered after adding an additional 10 wt% Carbon Black (CB) to SBCO

2.2.3 $SmBaCo_2O_{5+d}$ (SBCO) with $Ce_{0.9}Gd_{0.1}O_2$ (CGO91) specimens for electrical conductivity

SBCO powder was mixed with $Ce_{0.9}Gd_{0.1}O_2$ (CGO91, Rhodia) powder at a mass ratio of 0.5:1.5, 1:1, 1.5:0.5 and 1.9:0.1 . The mixed powders were charged into the metal mold and then were pressed with 2 x 10^3 kg/m^2 pressure. The pellets (25 mm x 6 mm x 4 mm) for the electrical conductivity measurement were sintered at 1150 ºC for 3 hours to investigate the composite effect on the SBCO_1150 sample, a sample showing higher conductivity values than other pure SBCO samples sintered at lower temperatures.

The composition ratio and abbreviations in SBCO with CGO91 cathode materials are summarized in Table 4.

Composition ratio (SBCO : CGO91)	Abbreviation
0.5 : 1.5	SBCO_0.5
1 : 1	SBCO_1
1.5 : 0.5	SBCO_1.5
1.9 : 0.1	SBCO_1.9

Table 4. Abbreviation of SBCO with CGO91 by composition ratio

2.2.4 Instrumentation and setup of electrical conductivity measurements

The electrical conductivities of all sample bars fabricated according to descriptions in 2.2.1 to 2.2.3 were measured using a DC 4 probe method with a Keithley 2400 Source Meter over a temperature range of 50 ~ 900 ˚C at steps of 50 ˚C and a heating rate of 5 ˚C/min. At each

temperature three different 4 terminal conductivity measurements were performed applying currents of 0.1, 0.5 and 1 A.

2.3 Microstructure analysis

After completion of the conductivity tests each sample was sputtered with Pt (Platinum), and the microstructures of the samples were observed at an acceleration voltage of 10 kV using a Scanning Electron Microscope (SEM, Model: HITACHI SU-5000) analyzing the images with the EM Wizard software. In addition, the particle size was calculated using the SEM images.

3. Results and discussion

3.1 Microstructural properties

X-ray Diffraction (XRD) results of $SmBaCo_2O_{5+d}$ (SBCO), which was synthesized by using Solid-State Reaction (SSR), are the same as those of SBCO reported by our group as a single phase [22]. Then, $SmBaCo_2O_{5+d}$ samples were sintered at 1000 ºC (SBCO_1000), 1050 ºC (SBCO_1050), 1100 ºC (SBCO_1100) and 1150 ºC (SBCO_1150) and microstructural properties of these samples were analyzed using a Scanning Electron Microscope (SEM)

The SEM results given in Fig. 1 show that the particle sizes of particles on the sample surface and of particles inside the sample increase with the sintering temperature applied to the samples, the increase in particle size results in an increased density of the microstructure. For example, the particle sizes of SBCO_1000, SBCO_1050, SBCO_1100 and SBCO_1150 were measured to be 2.89, 4.58, 4.71 and 6.54 μm in average, respectively.

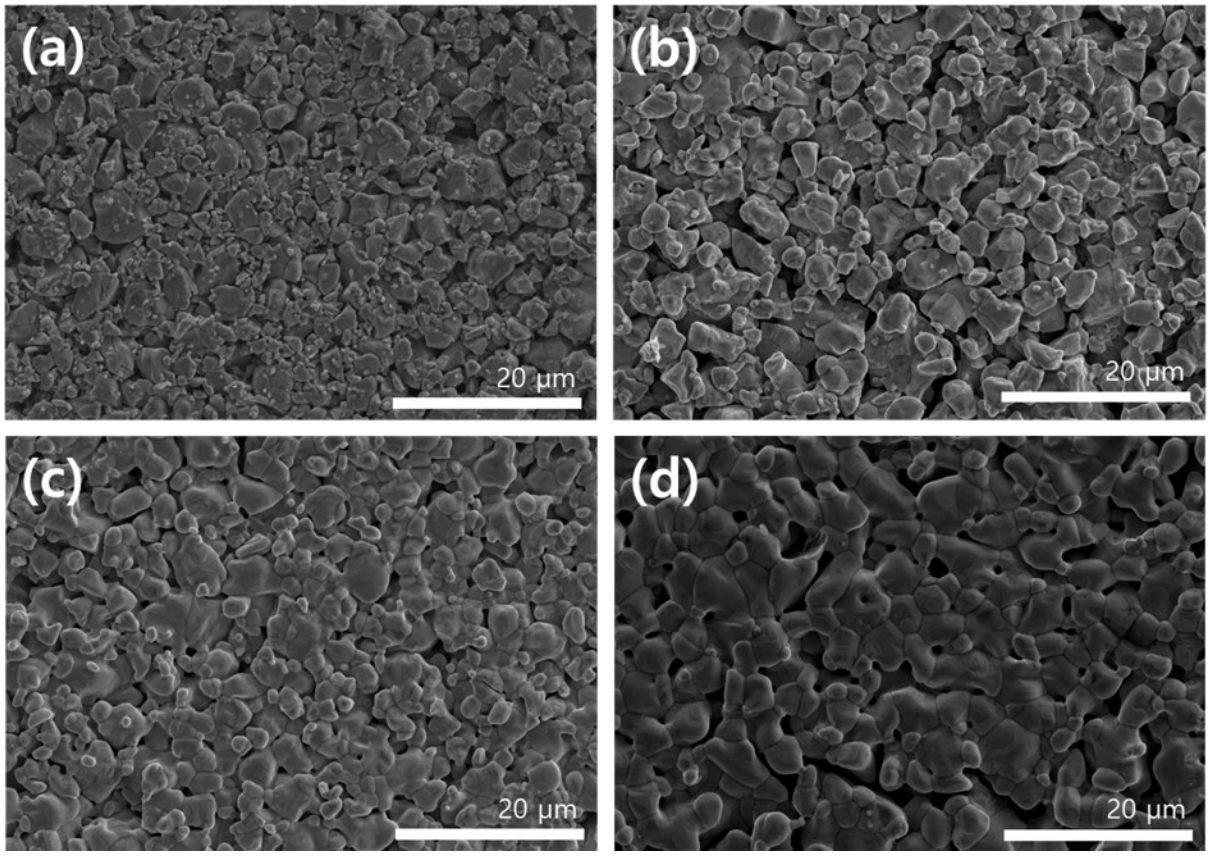

Fig. 1. Surface microstructural properties of (a) SBCO_1000, (b) SBCO_1050, (c) SBCO_1100, and (d) SBCO_1150.

Samples were prepared by adding excess Carbon Black (CB) to intentionally prepare porous structures while maintaining the bar-type shape. However, it was found that the mechanical strength of sample was so low that it was impossible to move and measure the sample when electrical conductivity samples using additional 10 wt% CB were sintered at 1000 ºC. Therefore, the samples mixed with SBCO and carbon black were sintered at 1050 ºC (SBCO10C_1050) instead of 1000 ºC

The surface SEM images of SBCO10C_1050 and SBCO10C_1150 are summarized in Fig. 2.

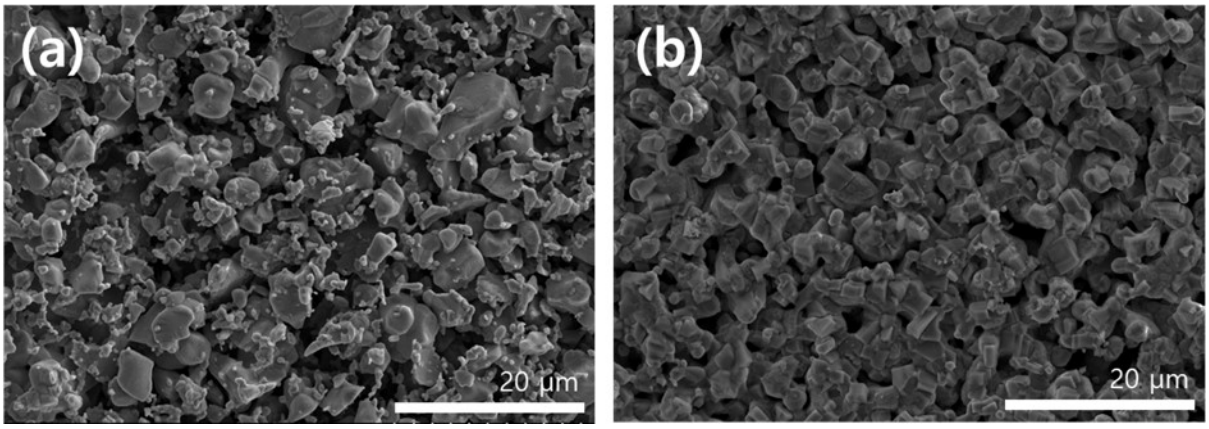

Fig. 2. Surface microstructural properties of (a) SBCO10C_1050 and (b) SBCO10C_1150. 10C in the sample name means that an additional 10wt% CB was included relative to the weight of SBSCO.

Even after mixing SBCO with CB, the microstructures become more dense as sintering temperature increases, as shown in Figures 2. (a) and (b). When comparing the results of Fig. 1. (b) with Fig. 2. (a), it can be seen that the microstructure becomes more porous when 10 wt% of CB are added to the sample under the same sintering temperature condition. Even when Fig. 1. (d) and Fig. 2. (b) are compared, the same characteristics can also be found. Generally, CB is known to be pyrolyzed at 1000 ºC [43] and these samples were sintered at 1050 ºC, which show the characteristics of the porous microstructure.

Fig. 3 shows SEM images of the surfaces of SBCO_1.5 and SBCO_1. The comparison of the two pictures shows microstructural changes occurring with an increasing share of CGO91 within the SBCO/CGO composite.

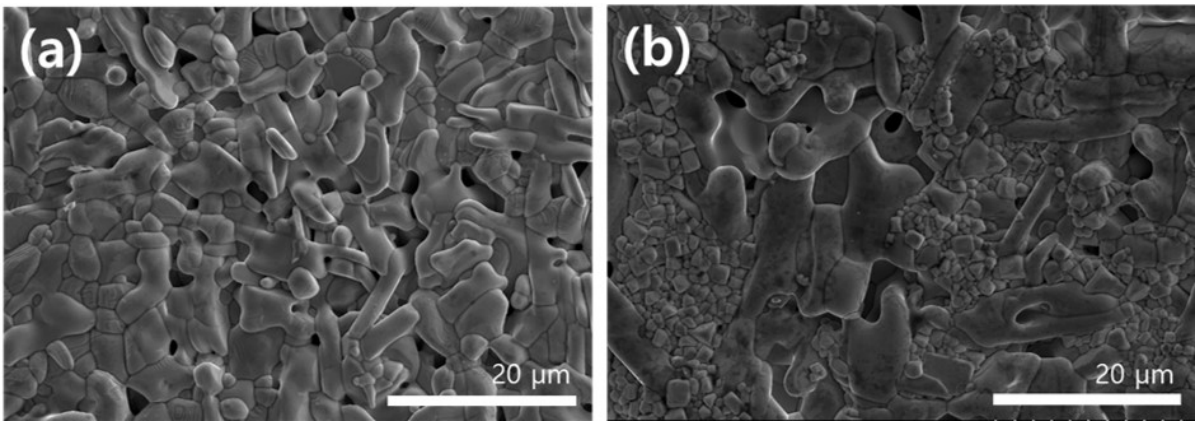

Fig. 3. Surface microstructural properties of (a) SBCO_1.5 and (b) SBCO_1.

According to Fig. 3. (a), a distinctive CGO91 phase can not be clearly identified in SBCO_1.5, a composition in which the ratio of SBCO is higher than that of CGO91. In this way Fig. 3. (a) appears very similar to the image of pure SBCO sintered at 1150 ºC depicted in Fig. 1. (d). However, if the composition ratio of CGO91 is equal or greater than 1:1, it can be seen that a large change appears in the microstructure and a lot of CGO91 can observed in the SEM image of SBCO_1 in Fig. 3. (b). As an additional observation related to this, the samples with a large amount of CGO91 (SBCO_1 and SBCO_0.5) showed similar electrical conductivity behavior as that of CGO91.

The electrical conductivity characteristics with respect to the various microstructures shown in Fig. 1, Fig. 2 and Fig. 3 will be explained in more detail in connection with the electrical conductivity results in Section 3.2.

3.2. Electrical conductivity properties

3.2.1 Electrical conductivities of $SmBaCo_2O_{5+d}$ (SBCO) sintered at various temperatures

The electrical conductivities of SBCO_1000, SBCO_1050, SBCO_1100 and SBCO_1150 were measured to find out how the sintering related microstructure affects the electrical conductivity; the results are shown in Fig. 4. The electrical conductivities were also measured by applying currents of 1 A, 0.5 A and 0.1 A to the outermost two lines of the DC 4 probe.

The maximum and minimum electrical conductivity values of applying 1 A with respect to the temperature are summarized in Table 5.

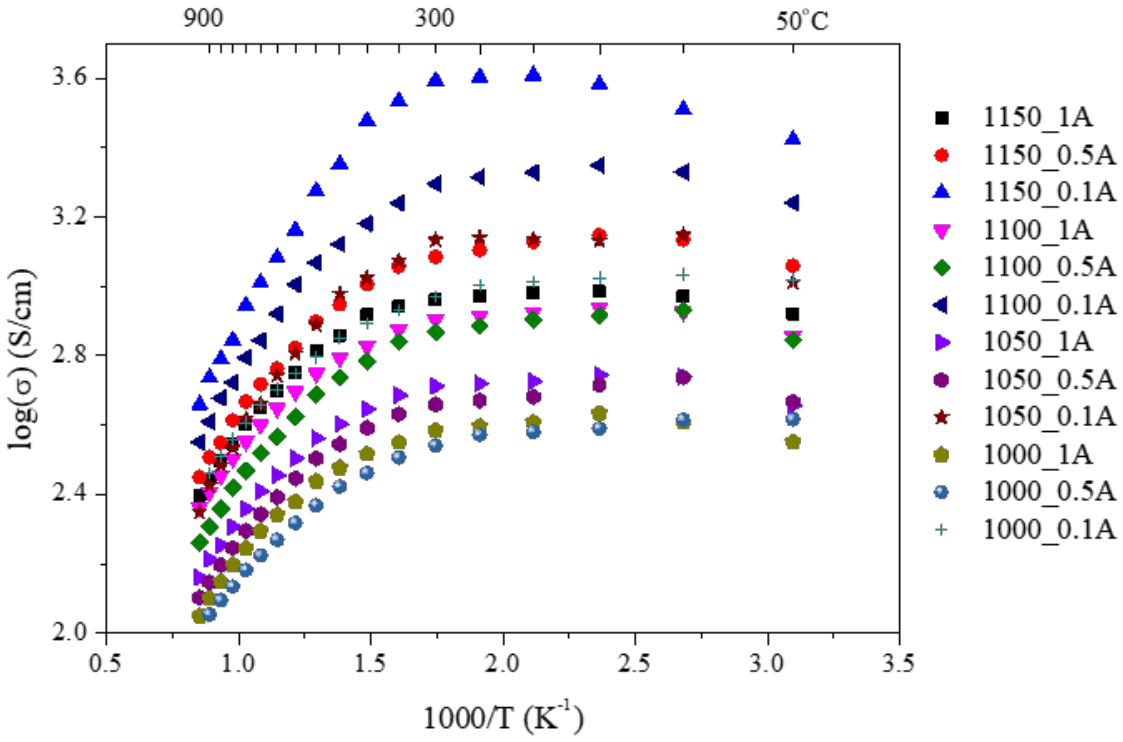

Figure 4. (a)

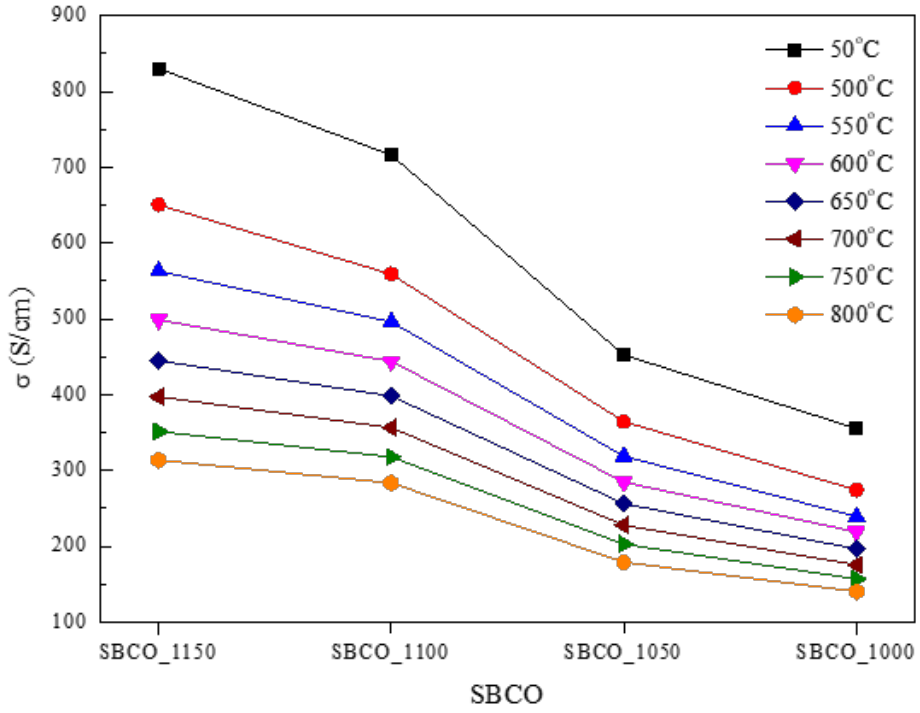

Fig. 4. (b)

Fig. 4. (a) Electrical conductivity results of applying 1, 0.5 and 0.1 A to the SBCO samples. (b) shows the summarized electrical conductivities of SBCO measured at a temperature of 50 ºC and in the temperature ranges of 500 ~ 800 ºC when a current of 1 A is applied to the SBCO samples.

Samples	Maximum conductivity (S/cm)	Temperature(ºC)	Minimum conductivity (S/cm)	Temperature(ºC)
SBCO_1000	430.3	150	112.1	900
SBCO_1050	554.7	150	144.2	900
SBCO_1100	862.1	150	229.6	900
SBCO_1150	962.6	150	249.1	900

Table 5. Maximum and minimum electrical conductivities of SBCO_1000, 1050, 1100, and 1150 measured at 150 and 900 ºC.

The overall electrical conductivity behaviors were summarized in Fig. 4; all samples show typical metal insulator transition (MIT) behavior, in which the electrical conductivity increases with increasing temperature at lower temperature ranges (50 ~ 300 ºC) and decreases with increasing temperature at a higher temperature range (300 ~ 900 ºC) [17]. This is mainly caused by the changed charge states of Co substituted into the B-site in the perovskite and can be explained with respect to the effect of temperatures. For example, the electrical conductivity increases in the low temperature range by increasing the concentration of Co^{4+} from the oxidation of Co^{3+} to Co^{4+}. However, the electrical conductivity decreases at temperatures above 150 ºC because the representative Co^{4+} charges, which increase the electrical conductivity, are saturated and at the same time the concentration of oxygen vacancies generated as a function of temperature increases which can also result in decrease of electrical conductivity [34].

According to the Table 5, the temperatures to show the maximum and minimum electrical conductivity were the same for all samples at 150 and 900 ºC. The maximum electrical conductivity was measured at a value of 962.6 S/cm in SBCO_1150 with the highest sintering

temperature. It can be determined that the higher the sintering temperature not only increases the density in samples, but also decreases the concentrations in grain boundary along with the growth of grains increasing the particle size through the sintering process.

According to results mentioned in Fig. 1 again, the particle sizes of SBCO_1000, SBCO_1050, SBCO_1100 and SBCO_1150 are 2.9, 4.6, 4.7 and 6.5 μm; the particle size of sample sintered at higher temperature is bigger than that of sample sintered at lower temperature. In other words, since the process of particle size growth is directly related to the decrease of grain boundary, the electrical conductivity increases because of a reduction of the length of the movement path of holes as the main charge carriers in Co substituted into B-site of layered perovskite or complex perovskite [35].

However, in the case of the lower sintering temperatures, the density of the grain boundaries is relatively increased, which results in a limited hole movement in the porous microstructure. Therefore, it can be determined that the lower sintering temperature, the lower the maximum electrical conductivity value in Fig. 3. (d). For example, SBCO_1000 sintered at the lowest temperature has the lowest minimum electrical conductivity at about 112.1 S/cm at 900 ºC.

To investigate the difference of electrical conductivity caused by different applied current densities, SBCO_1150 and SBCO_1000 were exposed to current strengths of 1 A, 0.5 A and 0.1 A using the DC 4 probe arrangement for electrical conductivity measurement; the results are shown in Fig. 5.

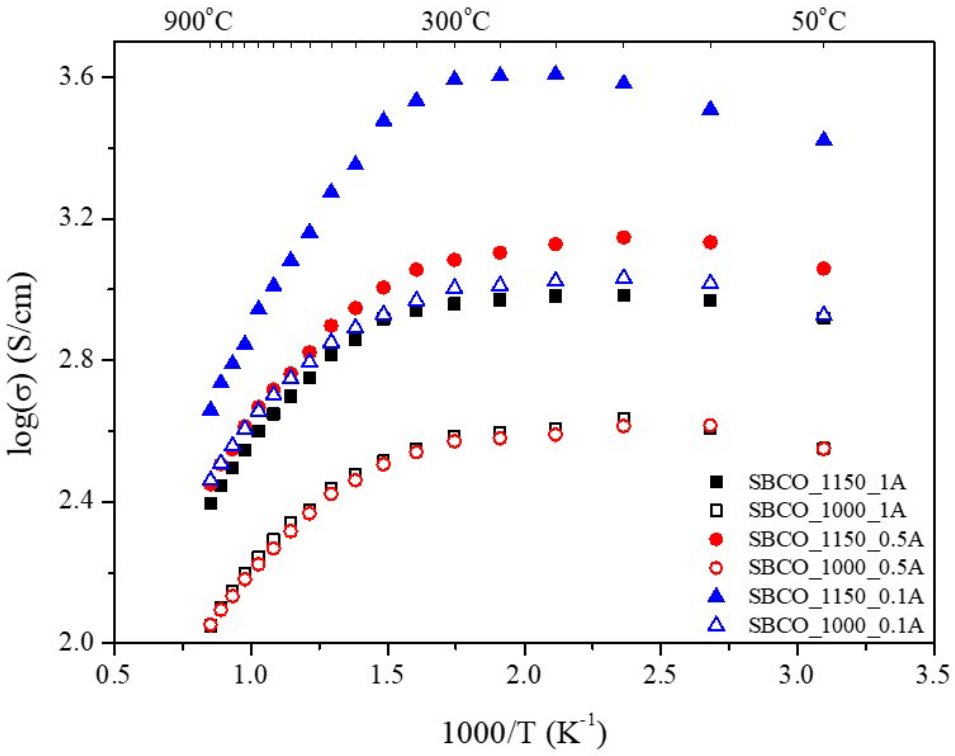

Fig. 5. Summaries of electrical conductivity of SBCO_1000 and SBCO_1150 when currents of 1 A, 0.5 A and 0.1 A were applied.

The values of electrical conductivity of SBCO_1150 with applied currents of 1 A, 0.5 A and 0.1 A were 445.1, 521.3 and 1024 S/cm at 600 ºC. At the same temperature and the same applied current conditions, SBCO_1000 showed electrical conductivities of about 197, 185 and 503 S/cm. These values show an inverse relation between the applied current strength and the measured conductivity values, a lower the applied current leads to a higher electrical conductivity. It can be determined that the measured voltage increase according to the applied current in the Co-substituted sample affects the electrical conductivity. According to Baek et al the decrease of electrical conductivity observed at higher current density can be explained by a reduction of the flux of internal charge carriers [36]. In the case of SBCO these charge carriers are electron holes created by the oxidation of Co^{+4} to Co^{+3}. At a higher current a larger number

of these charge carriers have to move through the same crystal lattice, the movement of the charge carriers is limited by the number of pathways in the lattice and the overall electrical conductivity is reduced.

3.2.2 Electrical conductivity of $SmBaCo_2O_{5+d}$ (SBCO) with 10 wt% Carbon black

To investigate the effect of a porous microstructure on the electrical conductivity, SBCO and 10 wt% carbon black were mixed and sintered at 1050 ºC (SBCO10C_1050) and 1150 ºC (SBCO10C_1150). The conductivity results at different current strengths are summarized in Fig. 6.

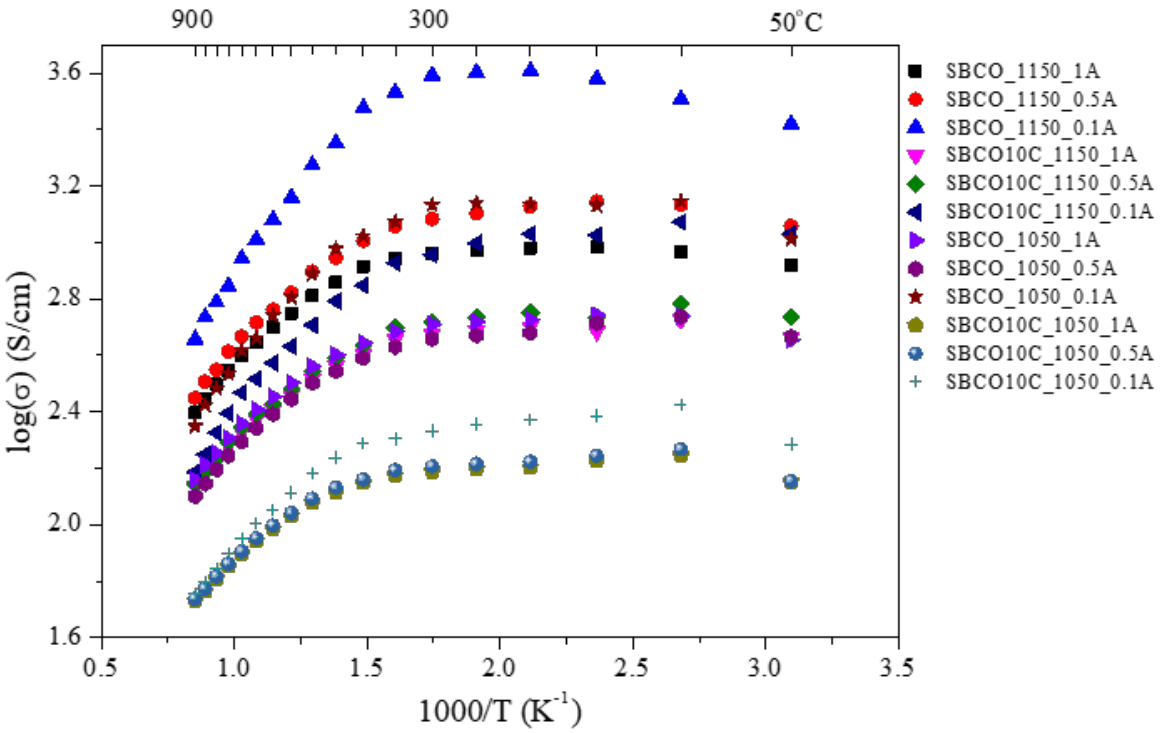

Fig. 6. Electrical conductivities of SBCO_1050, SBCO_1150, SBCO10C_1050, and SBCO10C_1150 when currents of 1, 0.5 and 0.1 A were applied.

3.2.2.1 Conductivity of porous samples

In summary, SBCO10C_1150 and SBCO10C_1050 artificially changed a dense structure into a porous structure suitable as a fuel cell electrode by addition of carbon black. As expected the added porosity results in a general decrease of electrical conductivity of the samples, with the extent of this decrease depending on the applied current.

As can be seen in Fig. 6, the porous samples SBCO10C_1150 and SBCO10C_1050 also showed the same MIT behavior as the dense samples SBCO_1150 and SBCO_1050, in which the electrical conductivity showed conductivity values increasing with increasing temperature at lower temperature ranges from 50 ºC to 150 ºC and decreasing conductivity values from 300 to 900 ºC. For most compositions and current strengths there is a plateau of maximum conductivity between roughly 150 ºC and 300 ºC, showing in Fig. 6 for porous samples in the same way as in Fig. 4 and Fig. 5 for dense samples .

The values for the electrical conductivity of SBCO_1150 were 499.0, 397.5 and 313.8 S/cm and those of SBCO10C_1150 were 256.6, 214.2 and 170.4 S/cm at 600, 700 and 800 ºC in the case of an applied current of 1 A. The value of electrical conductivity of SBCO_1150 at 600 ºC, is better than the values of $PrBa_{0.8}Ca_{0.2}Co_2O_{5+d}$ (197 S/cm), $GdBaCo_2O_{5+d}$ (about 400 S/cm), $PrBaCo_2O_{5+d}$ (about 200 S/cm) and $YBaCo_2O_{5+d}$ (20 S/cm) [34, 37-39]. In addition, the values of electrical conductivity of SBCO_1050 were 284.8, 228.2 and 179.1 S/cm and those of SBCO10C_1050 were 97.0, 79.1 and 64.6 S/cm at 600, 700 and 800 ºC with an applied current of 1 A.

These values show that the electrical conductivity decreases from the dense microstructure of the pure SBCO samples to the porous microstructure achieved by the addition of carbon black. This decrease of conductivity in porous samples is no surprise since the movement of charge carriers is limited by the pores in the porous structure [35]. The same trend is also shown in

Fig. 6 for smaller applied currents.

3.2.2.2 Suitable conductivity for IT-SOFC cathodes

Fig. 6 shows that the values of electrical conductivity in the temperature ranges of 600 ~ 800 ºC of SBCO10C_1150, which has the porous microstructure, are higher than 100 S/cm, which is the minimum electrical conductivity required for IT-SOFC cathodes [27, 40, 44]. On the other hand, the values of the electrical conductivity for SBCO10C_1050 were about 71 ~ 97 S/cm at 600 ~ 800 ºC, which does not satisfy the required minimum electrical conductivity for IT-SOFCs.

The porous sample sintered at higher temperature, SBCO10C_1150 and the dense sample sintered at lower temperature, SBCO_1050 exhibit similar electrical conductivity values. These conductivity values suggest that the decline in conductivity from the porous structure can be compensated by the increase of sintering temperature and grain size. Considering that cathodes of SOFCs need the microstructural characteristics of the porous structure for their functionality in gas transport, sufficient electrical conductivity values can be achieved by controlling the sintering temperature of the porous sample.

When applying various currents to SBCO10C_1050 and SBCO10C_1150, the same characteristics observed in Fig. 5 were also found in Fig. 6, namely that a lower current load generally results in better conductivity, no matter if the sample is dense or porous.

For the SBCO10C_1150 sample the values of electrical conductivity measured at applied currents of 1 A and 0.5 A were very similar 257 and 268 S/cm at 600 ºC . However, when a current of 0.1 A was applied to SBCO10C_1150, the value of electrical conductivity increased a lot to 375 S/cm at 600 ºC. This characteristic was also found in SBCO10C_1050. However, the electrical conductivity was generally lower lower than that of SBCO10C_1150.

3.2.2.3 The effect of porosity on the relation between sintering temperature and conductivity

On the first impression of the optical inspection of Fig. 6, the difference in electrical conductivity values between SBCO_1150 and SBCO_1050 seems smaller than between SBCO10C_1150 and SBCO10C_1050 in the diagram, but this is a deceptive effect of the logarithmic scale of the conductivity axis.

At the lower temperature (300 ºC), the electrical conductivity of the dense samples SBCO_1150 and SBCO_1050 were 911.8 and 515.0 S/cm, which shows a conductivity difference of 396.8 S/cm. The porous samples SBCO10C_1150 and SBCO10C_1050 with their porous microstructure show 474.9 and 155.0 S/cm with a conductivity difference of only 319.9 S/cm at the lower temperature 300 ºC, all values measured at an applied current of 1A. So, regarding to the absolute values, the positive effect of a higher sintering temperature is slightly less prominent in the samples with a porous microstructure.

The same trend shows at a relatively higher temperature (600 ºC). Electrical conductivity values of SBCO_1150 and SBCO_1050 were 499.0 and 284.8 S/cm showing a difference of 214.2 S/cm, the conductivities of SBCO10C_1150 and SBCO10C_1050 were measured to be 256.6 and 97.0 S/cm with a difference of 159.6 S/cm at an applied current 1A.

3.2.2.4 The effect of porosity on the relation between measured temperature and conductivity

As mentioned in chapter 3.2.2.1, a maximum conductivity of dense and porous SBCO samples can generally be achieved measuring the conductivity in the temperature range

between 150 ºC and 300 ºC. These temperatures are too low for electrode application in IT-SOFCs, a temperature of 600 ºC is more realistic, but under these higher temperatures the conductivity decreases.

Increasing the application temperature from 300 ºC to 600 ºC, will decrease the electrical conductivity of the SBCO_1150 sample by 412.8 S/cm or 45% of the maximum 911.8 S/cm and the electrical conductivity of SBCO_1050 by 230.2 S/cm or 45% of the maximum conductivity of 515 S/cm. The porous samples SBCO10_1150 and SBCO10_1050 shows 218.3 S/cm and 58 S/cm, 46% and 37% of their plateau conductivity, respectively, if you heat them from 300 ºC to 600 ºC. That is, the ranges of electrical conductivity values measured over different temperatures with dense samples is larger than those of the electrical conductivity values with porous samples in absolute numbers, but similar or even slightly smaller in percentage of the maximum conductivity .

3.2.3 Electrical conductivity of composite cathodes comprised of SBCO and $Ce_{0.9}Gd_{0.1}O_2$ (CGO91)

Fig. 7 shows the electrical conductivity results of composite cathodes comprised of SBCO and $Ce_{0.9}Gd_{0.1}O_2$ (CGO91) at a mass ratio 0.5:1.5 (SBCO_0.5), 1:1 (SBCO_1), 1.5:0.5 (SBCO_1.5), and 1.9:0.1 (SBCO_1.9) at the temperature ranges between 50 and 900 ºC with interval of 50 ºC.

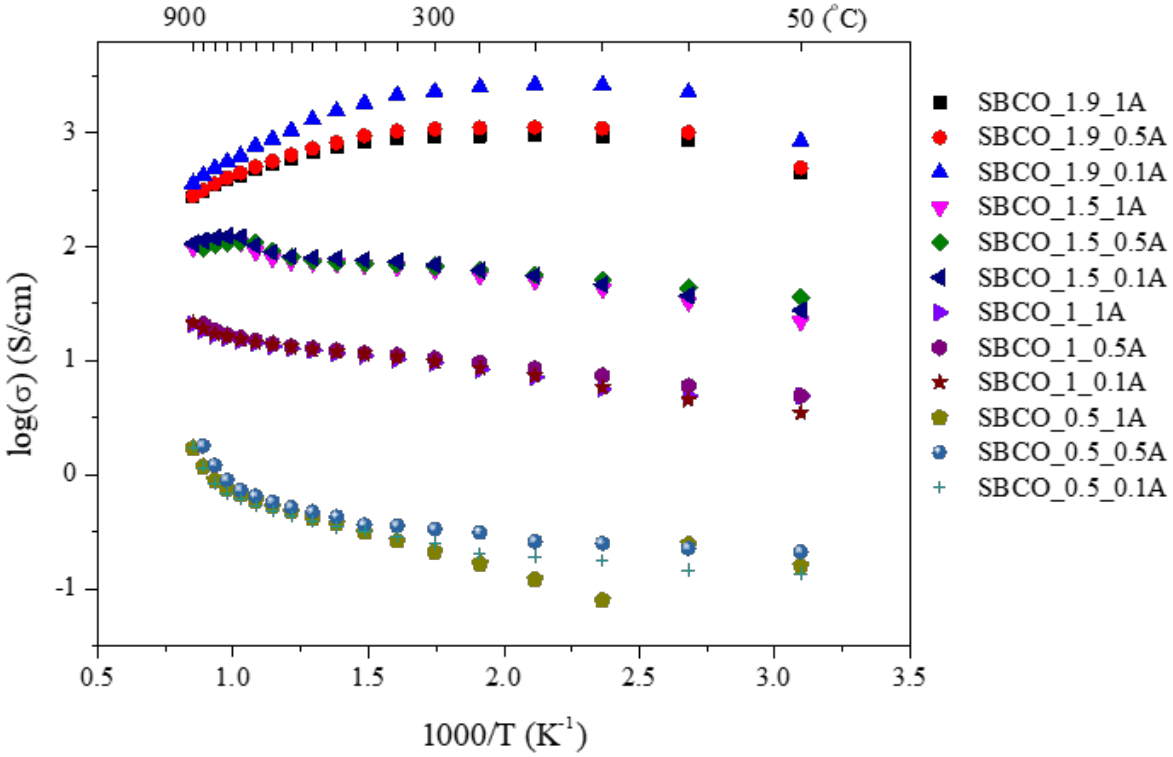

Fig. 7. Electrical conductivities of SBCO_1.9, SBCO_1.5, SBCO_1, and SBCO_0.5 when currents of 1, 0.5 and 0.1 A were applied.

As can be seen in Fig. 7, the SBCO_1.9 sample shows the typical MIT behavior with a plateau of maximal conductivity in the temperature range between 150 ºC and 300 ºC, the same as the pure SBCO samples [17, 31]. It is not a surprise that this sample behaves similar to SBCO, since this sample has the highest SBCO content of 95%. However, the temperature dependence of electrical conductivity changes with increasing content of CGO91. SBCO_0.5, the sample with the lowest SBCO content (25%) and highest CGO content (75%), showed a similar conductivity behavior to CGO91, with significantly lower conductivities at lower temperature ranges measured [41, 42]. As the content of SBCO increases in composite cathodes, the temperature dependency of conductivity behavior of the composite cathode is close to that of single phase SBCO, but as the content of CGO91 increases, the conductivity behavior

increasingly follows the conductivity behavior of CGO91.

From Fig. 7, the values of electrical conductivity of SBCO_0.5, SBCO_1, SBCO_1.5 and SBCO_1.9 were measured to be 0.213, 9.59, 62.7 and 90.9 S/cm at 300 ºC, and 1.725, 20.82, 98.89 and 272.9 S/cm at 900 ºC based on the applied current of 1A. Fig. 7 clearly shows that the electrical conductivity of composite samples consisting of SBCO and CGO91 decreases with increasing CGO91 content, this is true for all temperatures and for all current loads applied. The electrical conductivity values are particularly bad if the composition ratio of CGO91 is greater than 0.5.

In the case of a composite cathode comprised of CGO91 as the ionic conductor on SBCO as the mixed ion-electron conductor (MIEC), the movements of the holes, which are the main charge carrier in these materials, are hindered by CGO91, and at the same time, the activation energy increases with increasing CGO content, which results in the decreased electrical conductivity value [41, 42].

When comparing only the electrical conductivity values measured to the minimum electrical conductivity (100 S/cm) for IT-SOFCs, SBCO_1.9 exceeds 100 S/cm in all measured temperature ranges and SBCO_1.5 exceeds 100 S/cm at temperatures above 700 ºC. SBCO_0.5 and SBCO_1 do not satisfy the minimum electrical conductivity value at any temperature [44, 45], and once further decrease because of porosity is taken into account, also SBCO_1.5 doesn't seem suitable as cathode material for IT-SOFCs.

Comparing data of Fig 7, SBCO_0.5, SBCO_1 and SBCO_1.5 showed low electrical conductivity values at all currents applied and the conductivity dependency on the applied current was found insignificant, in other words the conductivity values were similarly low whether 0.1A, 0.5A or 1A current loads were applied. However, SBCO_1.9 shows a large dependence of the electrical conductivity value on the applied current in the way that the conductivity is much higher at a lower current load. For example, SBCO_0.5 shows electrical

conductivities of 0.48, 0.51, and 0.53 S/cm at applied currents of 0.1, 0.5 and 1 A at 600 ºC as summarized in Fig. 7. However, SBCO_1.9 shows high electrical conductivity values of 884.00, 559.60, and 525.37 S/cm at the same temperature and applied current condition, conductivity showing a clear current dependency.

Through this, there is a big difference between the conductivity result of the single phase summarized in Sections 3.2.1 and 3.2.2 and the conductivity tendency of the composite phase presented in this section 3.2.3. In summary, the conductivity value does not significantly improve in the composite cathode mixed with CGO91 under a low current condition**.**

Conclusion

In this research work $SmBaCo_2O_{5+d}$ (SBCO) was investigated as a material for IT-SOFC cathodes, both as a single phase and as a component in a composite material with CGO91. Microstructural changes as a result of different sintering temperatures and of induced porosity by adding 10% carbon and their effect on the overall electrical conductivity values were studied.

With increasing sintering temperature of SBCO the particle size generally increases and the microstructure becomes denser and coarser.

The conductivity of samples sintered at 1000, 1050, 1100 and 1150 ºC showed metal insulator transition (MIT) behavior. The values of electrical conductivity of SBCO_1150 and SBCO_1000 were measured at 445.1 and 196.7 S/cm at 600 ºC. SBCO of the same composition shows an increase of electrical conductivity by about a factor two or more as the sintering temperature increases because the main charge carriers can move freely without being isolated in the denser microstructure.

Electrical conductivities of SBCO10C_1150 and SBCO10C_1050, which increased porosity by mixing CB, were measured at 256.6 and 97.0 S/cm at 600 ºC, which shows that the electrical

conductivity generally decreases as porosity increases.

SBCO10C_1150 and SBCO_1050 are different in porosity and density but show similar electrical conductivity values. Clearly electrical conductivity values can be controlled by both changing the sintering temperature and the porosity of the sample.

The values of electrical conductivity of SBCO_1.9 were 909.31 and 272.89 S/cm at 300 and 900 ºC (applied current 1A), better than the values of SBCO_0.5, SBCO_1 and SBCO_1.5 samples. Also, the electrical conductivity of SBCO_1.9 is higher than 100 S/cm at all relevant temperatures, exceeding the minimum electrical conductivity required for IT-SOFC. However, with the ratio of CGO91 increasing in the SBCO/CGO composite cathodes, the value of electrical conductivity rapidly decreases.

Generally the electrical conductivity improved as the applied current decreased, this effect could be observed at dense and porous SBCO samples of all sintering temperatures. On the other hand, the above-mentioned phenomenon did not appear in composite cathodes of SBCO and CGO91 with a CGO content higher than 5%.

Acknowledgements

This work was supported by the National Research Foundation of Korea (NRF) grant funded by the Korean government (MSIT) (No. 2019R1A2C1087534).

Reference

[1] M. Anderson, J. Yuan, B. Sunden. SOFC modeling considering hydrogen and carbon monoxide as electrochemical reactants. J Power Sources, 232 (2013), p. 42-54, 10.1016/j.jpowsour.2012.12.122

[2] M.A. Abdelkareem, K. Elsaid, T. Wilberforce, M. Kamil, E.T. Sayed, A. Olabi. Environmental aspects of fuel cells: a review. Sci Total Environ, 752 (2020), p. 141803, 10.1016/j.scitotenv.2020.141803

[3] F.S. da Silva, T.M. de Souza. Novel materials for solid oxide fuel cell technologies: a literature review. Int J Hydrogen Energy, 42 (2017), p. 26020-26036, 10.1016/j.ijhydene.2017.08.105

[4] B.C.H. Steele, A. Heinzel. Materials for fuel-cell technologies. Nature, 414 (2001), p. 345-352, 10.1142/9789814317665_0031

[5] A.W. Martin, A.M. Ruiz, M.A. Laguna-Bercero, R. Campana, A. Larranaga, P.R. Slater, M.I. Arriortua. SOFC cathodic layers using wet powder spraying technique with self synthesized nanopowders. Int J Hydrogen Energy, 44 (2019), p. 7555-7563, 10.1016/j.ijhydene.2019.01.220

[6] A.M. Nassef, A. Fathy, E.T. Sayed, M.A. Abdelkareem, H. Rezk, W.H. Tanveer, A.G. Olabi. Maximizing SOFC performance through optimal parameters identification by modern optimization algorithms. Renewable Energy, 138 (2019), p. 458-464, 10.1016/j.renene.2019.01.072

[7] S. Inac, S.O. Unverdi, A. Midilli. A parametric study on thermodynamic performance of a SOFC oriented hybrid energy system. Int J Hydrogen Energy, 44 (2019), p. 10043-10058, 10.1016/j.ijhydene.2019.01.247

[8] A. Weber, E.I. Tiffee. Materials and concepts for solid oxide fuel cells (SOFCs) in stationary and mobile applications. J Power Sources, 127 (2004), p. 273-283,

10.1016/j.jpowsour.2003.09.024

[9] S.W. Song, W.S. Choi, H. Kang, S.W. Baek, A.K. Azad, J.Y. Park, J.H. Kim. Synthesis and electrochemical properties of layered perovskite substituted with heterogeneous lanthanides for intermediate temperature-operating solid oxide fuel cell. Int J Hydrogen Energy, 43 (2018), p. 11378-11385, 10.1016/j.ijhydene.2018.04.011

[10] J. Molenda, K. Swierczek, W. Zaja. Functional materials for the IT-SOFC. J Power Sources, 173 (2007), p. 657-670, 10.1016/j.jpowsour.2007.05.085

[11] E. Fabbri, L. Bi, D. Pergolesi, E. Traversa. Towards the next generation of solid oxide fuel cells operating below 600 ºC with chemically stable proton-conducting electrolytes. Adv Mater, 24 (2012), p. 195-208, 10.1002/adma.201103102

[12] L. Miao, J. Hou, Z. Gong, Z. Jin, W. Liu. A high-performance cobalt-free Ruddlesden-Popper phase cathode $La_{1.2}Sr_{0.8}Ni_{0.6}Fe_{0.4}O_{4+\delta}$ for low temperature proton-conducting solid oxide fuel cells. Int J Hydrogen Energy, 44 (2019), p. 7531-7537, 10.1016/j.ijhydene.2019.01.255

[13] W. Ni, T. Zhu, X. Chen, Q. Zhong, W. Ma. Stable, efficient and cost-competitive Ni-substituted $Sr(Ti,Fe)O_3$ cathode for solid oxide fuel cell: effect of A-site deficiency. J Power Sources, 451 (2020), p. 227762, 10.1016/j.jpowsour.2020.227762

[14] J. Chen, D. Wan, X. Sun, B. Li, M. Lu. Electrochemical impedance spectroscopic characterization of impregnated $La_{0.6}Sr_{0.4}Co_{0.2}Fe_{0.8}O_{3-\delta}$ cathode for intermediate-temperature SOFCs. Int J Hydrogen Energy, 43 (2018), p. 9770-9776, 10.1016/j.ijhydene.2018.03.223

[15] N. Ai, S. He, N. Li, Q. Zhang, W.D. Rickard, K. Chen, T. Zhang, S.P. Jiang. Suppressed Sr segregation and performance of directly assembled $La_{0.6}Sr_{0.4}Co_{0.2}Fe_{0.8}O_{3-\delta}$ oxygen electrode on Y_2O_3-ZrO_2 electrolyte of solid oxide electrolysis cells. J Power Sources, 384 (2018), p. 125-

135, 10.1016/j.jpowsour.2018.02.082

[16] M.Z. Khan, M.T. Mehran, R.H. Song, S.B. Lee, T.H. Lim. Effects of applied current density and thermal cycling on the degradation of a solid oxide fuel cell cathode. Int J Hydrogen Energy, 43 (2018), p. 12346-12357, 10.1016/j.ijhydene.2018.04.175

[17] J.H. Kim. Comparison of Electrical Conductivities in Complex Perovskites and Layered Perovskite for Cathode Materials of Intermediate Temperature-operating Solid Oxide Fuel Cell. J Korean Ceram Soc, 51 (2014), p. 295-299, 10.4191/kcers.2014.51.4.295

[18] A.A. Taskin, A.N. Lavrov, Y. Ando. Fast Oxygen Diffusion in A-site Ordered Perovskites, Pro. Solid State Chem, 35 (2007), p. 481-490, 10.1016/j.progsolidstchem.2007.01.014

[19] S.H. Woo, T.H. Shin, H. Kang, W.S. Choi, H.S. Kim, J.H. Kim. Phase Synthesis and Electrochemical Characteristics of Non-stoichimometric $Sm_{1-x}Ba_{0.5}Sr_{0.5}Co_2O_{5+d}$ Layered Perovskites for IT-SOFC Cathodes. New & Renewable Energy, 15 (2019) p. 81-89, 10.7849/ksnre.2019.6.15.2.081

[20] Y.H. Joung, H. Kang, W.S. Choi, J.H. Kim. Investigation of X-Ray Photoelectron Spectroscopy and Electrical Conductivity Properties of the Layered Perovskite $LnBaCo_2O_{5+d}$ (Ln = Pr, Nd, Sm, and Gd) for IT-SOFC. Electron Mater Lett, 9 (2013), p. 463-465, 10.1007/s13391-013-0002-8

[21] S.W. Baek, A.K. Azad, J.T.S. Irvine, W.S. Choi, H. Kang, J.H. Kim. Electrochemical properties of composite cathodes using Sm doped layered perovskite for intermediate temperature-operating solid oxide fuel cell. Appl Surf Sci, 432 (2018), p. 272-277, 10.1016/j.apsusc.2017.02.211

[22] J.H. Kim, Y.M. Kim, P.A. Connor, J.T.S. Irvine, J.M. Bae, W. Zhou. Structural, thermal and electrochemical properties of layered perovskite $SmBaCo_2O_{5+d}$, a potential cathode

material for intermediate-temperature solid oxide fuel cells. J Power Sources, 194 (2009), p. 704-711, 10.1016/j.jpowsour.2009.06.024

[23] Y. Quan, T. Dong, L. Rui, W. Haodong, C. Yonghong, D. Yanzhi, L. Xiaoyong, L. Bin. Exploiting rare-earth-abundant layered perovskite cathodes of $LnBa_{0.5}Sr_{0.5}Co_{1.5}Fe_{0.5}O_{5+d}$ (Ln=La and Nd) for SOFCs. Int J Hydrog, 46 (2021), p. 5630-5641, 10.1016/j.ijhydene.2020.11.031.

[24] Z. Ling, N. Qiong, H. Beibei, L. Bin. Novel layered perovskite oxide $PrBaCuCoO_{5+d}$ as a potential cathode for intermediate-temperature solid oxide fuel cells. J Power Sources, 195 (2010), p. 453-6, 10.1016/j.jpowsour.2009.08.009

[25] X. Kong, G. Liu, Z. Yi, X, Ding. $NdBaCu_2O_{5+d}$ and $NdBa_{0.5}Sr_{0.5}Cu_2O_{5+d}$ layered perovskite oxides as cathode materials for IT-SOFCs. Int J Hydrog, 40 (2015), p. 16477-16483, 10.1016/j.ijhydene.2015.09.006

[26] K.E. Song, S.H. Woo, S.W. Baek, H. Kang, W.S. Choi, J.Y. Park, J.H. Kim. $SmBa_{1-x}Ca_xCo_2O_{5+d}$ Layered Perovskite Cathodes for Intermediate Temperature-operating Solid Oxide Fuel Cells. Front Chem, 9 (2021), p. 628823, 10.3389/fchem.2020.628813.

[27] S.W. Song, W.S. Choi, H. Kang, S.W. Baek, A.K. Azad, J.Y. Park, J.H. Kim. Synthesis and electrochemical properties of layered perovskite substituted with heterogeneous lanthanides for intermediate temperature-operating solid oxide fuel cell. Int J Hydrog, 43 (2018), p. 11378-11385, 10.1016/j.ijhydene.2018.04.011

[28] X. Lu, B. Tjaden, A. Bertei, T. Li, K. Li, D. Brett, P. Shearing. 3D characterization of diffusivities and its impact on mass flux and concentration overpotential in SOFC anode. J Electrochem Soc, 164 (2017), p. F188-F195, 10.1149/2.0111704jes

[29] X. Zhana, M. Espinoza, T. Li, M. Andersson. Parametric study for electrode microstructure

influence on SOFC performance. 46 (2021), p. 37440-37459, 10.1016/j.ijhydene.2021.09.057

[30] P.R. Shearing, Q. Cai, J.I. Golbert, V. Yufit, C.S. Adjiman, N.P. Brandon. Microstructural analysis of a solid oxide fuel cell anode using focused ion beam techniques coupled with electrochemical simulation. J Power Sources, 195 (2010), p. 4804-4810, 10.1016/j.jpowsour.2010.02.047

[31] Q. Zhou, T. He, Y. Ji. $SmBaCo_2O_{5+d}$ double-perovskite structure cathode material for intermediate-temperature solid-oxide fuel cells. J Power Sources, 185 (2008), p. 754-758, 10.1016/j.jpowsour.2008.07.064.

[32] K.S. Lee, D.W. Seo, J.H. Yu, S.K. Woo. A study on the Improvement of Strength in NiO-YSZ Porous Anode Material for Solid Oxide Fuel Cell. J Korean Ceram Soc, 40 (2003), p. 241-248. 10.4191/KCERS.2003.40.3.241

[33] J.H. Noh, J.H. Myung. Optimization of anode and electrolyte microstructure for Solid Oxide Fuel Cells. 57 (2019), p. 525-530, 10.9713/kcer.2019.57.4.525

[34] J.H. Kim, M. Cassidy, J.T.S. Irvine, J.M. Bae. Electrochemical investigation of composite cathodes with $SmBa_{0.5}Sr_{0.5}Co_2O_{5+d}$ cathodes for intermediate temperature operating solid oxide fuel cell. Chem Mater, 22 (2010), p. 883-892, 10.1021/cm901720w

[35] A.A. Samat, A.A. Jais, M.R. Somalu, N. Osman, A. Muchtar, K.L. Lim. Electrical and electrochemical characteristics of $La_{0.6}Sr_{0.4}CoO_{3-\delta}$ cathode materials synthesized by a modified citrate-EDTA sol-gel method assisted with activated carbon for proton-conducting solid oxide fuel cell application. J Sol-Gel Sci Tech, 86 (2018), p. 617-630, 10.1007/s10971-018-4675-1

[36] K.S. Baek, S.W. Baek, H. Kang, W.S. Choi, J.Y. Park, S. Saxin, S.K. Lee, J.H. Kim. Electrical conductivity characteristics of Sr substituted layered perovskite cathode ($SmBa_{0.5}Sr_{0.5}Co_2O_{5+d}$) for intermediate temperature-operating solid oxide fuel cell. Ceram,

(2022), 10.1016/j.ceramint.2022.02.114

[37] C. Lim, S. Sengodan, D. Jeong, J.Y. Shin, G.T. Kim. Investigation of the Fe doping effect on the B-site of the layered perovskite $PrBa_{0.8}Ca_{0.2}Co_2O_{5+d}$ for a promising cathode material of the intermediate-temperature solid oxide fuel cells. Int J Hydrog Energy, 44 (2019), p. 1088-1095, 10.1016/j.ijhydene.2018.10.182

[38] N. Li, Z. Lü, B. Wei, X. Huang, K. Chen, Y. Zhang, W. Su. Characterization of $GdBaCo_2O_{5+\delta}$ cathode for IT-SOFCs. J Alloys Compd, 454 (2008), p. 274-279, 10.1016/j.jallcom.2006.12.017

[39] L. Zhao, B. He, B. Lin, H. Ding, S. Wang, Y. Ling, R. Peng, G. Meng, X. Liu. High performance of proton-conducting solid oxide fuel cell with a layered $PrBaCo_2O_{5+\delta}$ cathode. J Power Sources, 194 (2009), p. 835-837, 10.1016/j.jpowsour.2009.06.010

[40] E. Boehm, J.M. Bassat, M.C. Steil, P. Dordor, F. Mauvy, J.C. Grenier. Oxygen transport properties of $La_2Ni_{1-x}Cu_xO_{4+\delta}$ mixed conducting oxides. Solid State Sci, 5 (2003), p. 973-981, 10.1016/S1293-2558(03)00091-8.

[41] H.Y. Lee, B.K. Kang, H.C. Lee, Y.W. Heo, J.J. Kim, J.H. Lee. Effects of Co-doping on Densification of Gd-doped CeO_2 Ceramics and Adhesion Characteristics on a Yttrium Stabilized Zirconia Substrate. J Korean Ceram Soc, 55 (2018), p. 576-580, 10.4191/kcers.2018.55.6.05

[42] A.K. Baral, H.P. Dasari, B.K. Kim, J.H. Lee. Effect of sintering aid (CoO) on transport properties of nanocrystalline Gd doped ceria (GDC) materials prepared by co-precipitation method. J Alloy Compd, 575 (2013), p. 455-460, 10.1016/j.jallcom.2013.05.191

[43] B.H. Kim, S.H. Kim, E.S. Choi. Preparation and properties of porous $(Ca, Mg)_{0.15}Zr_{0.7}O_{1.7}$ ceramics. J Korean Cryst Growth Cryst Technol, 21 (2011), p. 70-74,

10.6111/JKCGCT.2011.21.2.070

[44] H.Y. Tu, Y. Takeda, N. Imanishi, O. Yamamoto. $Ln_{1-x}Sr_xCoO_3$(Ln = Sm, Dy) for the electrode of solid oxide fuel cells. Solid State Ion, 100 (1997), p. 283-288, 10.1016/S0167-2738(97)00360-3

[45] S. Carter, A. Selcuk, R.J. Chater, J. Kajda, J.A. Kilner, B.C.H. Steele. Oxygen Transport in Selected Nonstoichiometric Perovskite-structure Oxides. Solid State Ion, 53 (1992), p. 597-605, 10.1016/0167-2738(92)90435-R